ISSN 0029-3865

CBPF-NF-006/89

EPR STUDIES OF PHOTOLYSIS OF HbNO AT LOW TEMPERATURES

by

Marília P. LINHARES[1+], Léa J. EL-JAICK[1*],
George BEMSKI[1] and Eliane WAJNBERG[1]

[1]Centro Brasileiro de Pesquisas Físicas - CBPF/CNPq
Rua Dr. Xavier Sigaud, 150
22290 - Rio de Janeiro, RJ - Brasil

[+]Permanent address:
Instituto de Física
Universidade Federal do Rio de Janeiro
Ilha do Fundão
21910 - Rio de Janeiro, RJ - Brasil

*To whom correspondence should be addressed.

Abstract: Photolysis of HbNO has been studied below 20K by electron spin ressonance at continuous illumination. Non exponential kinetics of both dissociation and reassociation of NO have yielded a consistent picture of NO tunneling to probably more than one site distant less than 0.1nm from the bound position. This result is obtained using the model of conformational substates or a model of a sum of two exponentials.

Key-words: Photolysis of HbNO; EPR of HbNO; Hemoproteins at low temperatures.

I. Introduction

The process of recombination of carbon monoxide (CO) to the heme in myoglobin (Mb) and to the hemes of the isolated chains of hemoglobin (Hb) has been studied by Frauenfelder et al.[1] by microsecond laser flash photolysis using optical absorption and infrared measurements. It has been shown that at temperatures below 200K the reassociation of ligands after the flash, is geminate and not exponential in time. This was attributed to a non homogeneity of the frozen population of molecules reflected by a distribution, g(E), of the activation energies (enthalpy) for the ligand reasssociation. As a result, the kinetics follow a power law. Recently another model interprets the reaction dynamics in terms of vibrational modes[2] in the protein.

Dissociation of CO and O_2 in Mb and Hb has been observed at high temperatures by fast spectroscopic techniques[3] after femto, pico and nano second laser pulse photolysis before the proteins relax to the stable deoxy conformation. In these experiments the transient spectra of intermediate species have been identified, in contrast to the kinetic approaches of the low temperature experiments.

At low temperatures it is possible to isolate the intermediate steps of the reactions following the photodissociation. The low temperature photoproduct is the same that is generated transiently at room temperature[4]. The geminate process which occurs at low temperature can occur at room temperature.

Photolysis depends on the protein and on the ligand[5]. Investigations with different ligands and with modified proteins[6] are important to verify conformational effects; use of other techniques besides the optical ones[7] (Raman, infrared spectroscopy and optical absorption) is helpful in extending our understanding of these complicated processes.

Hb and Mb recombination with NO ligand at room temperature have been observed by optical absorption[8]. Since nitrosyl heme compounds have an odd electron spin (S = 1/2), the Electron Paramagnetic Ressonance (EPR) technique can also be used in these compounds studies[9].

Nagai et al.[10] observed NO photodissociation in Hb, isolated chains and hybrids of Hb by EPR at T = 4.2K. Reassociation was not observed at this temperature.

Doetschman and Utterbach[11] described photodissociation in HbNO crystals at T = 1.7K and observed the thermal reassociation only at T > 70K. NO-cytochrome c oxidase photolysis was also studied by EPR and the kinetic curves were fitted according to the conformational substate model[12].

In this work we use EPR to analyze the recombination of NO to human Hb during and after photolysis with continuous illumination below T = 20K. The ligand recombination rates were determined under two different experimental conditions: with light on and in the dark.

Our experimental kinetic curves can be fitted under various assumptions; with the energy distribution in the conformational substates model[1a], including the hypothesis of recombination via quantum-mechanical tunneling[1b] or with a sum of

two exponentials[4c].

II. Material and Methods

Hemoglobin solution (Hb) was obtained by hemolysis of human blood, and was stripped of ions by passage through a sephadex G-25 (Sigma Co.) column. The solution was diluted to a 0.2mM heme concentration with a 0.1M phosphate buffer, pH 6.5. Nitrosyl hemoglobin (HbNO) was prepared as described by Louro et al.[9a] . The Hb samples were left to equilibrate with nitric oxide for at least 2 hours before freezing.

A helium flux cryostat (Helitran LTD-3-110) with a APD-E temperature controller (both from Air Products and Chemical) were used to control the sample temperature. Temperatures were measured with a Au-Fe versus Chromel thermocouple placed on the sample tube wall. Temperatures were stable to within 1K.

EPR experiments were performed with a X-band spectrometer (Varian E-9). Spectra were obtained at low microwave power ($\approx$ 2mW) to avoid saturation effects and with 2.0G modulation amplitude.

Photodissociation experiments were performed illuminating the sample through the window of the EPR cavity, with a 1000W Xenon Arc Lamp (Oriel Corp. of America Stanford) collimated and filtered through a saturated copper sulphate solution. A dissociation rate of $0.04s^{-1}$ was estimated considering the geometry and the filter characteristics. The light was left on for a time long enough for the EPR signal to reach steady state.

Figure 1 shows, as example, the EPR spectra of a HbNO

sample at 7.2K before photolysis, S_o, and during illumination at steady state, S_∞. The reassociation is then observed after blocking the light with a screen. Before repeating the experiment at a different temperature, the sample was warmed to 77K so that the EPR signal intensity was recovered.

Curves of Figure 2 show the time dependence of the HbNO EPR intensity $\Delta I(t)$ at g = 1.98 (indicated by arrow on Figure 1) during and after illumination. These curves were digitalized at intervals of 0.6s and normalized to the equilibrium values at each temperature:

$$N_{L,D}(t) = \frac{I_o - I_{L,D}(t)}{I_o - I_\infty} \qquad (1)$$

$N_{L,D}(t)$ is proportional to the fraction of unbound NO molecules during the illumination and in the dark. I_o is the EPR signal intensity at g = 1.98 before photolysis and I_∞, the steady state value during illumination. $\Delta I_{L,D}(t) = I_o - I(t)$ is directly obtained from Figure 2. The normalized experimental curves are shown in Figure 3. The experimental errors are estimated at maximum 10%.

During the illumination the experimental steady state fraction of dissociated ligands, at each temperature, can be obtained either from the EPR line amplitudes, $F_L(\infty) = (I_o - I_\infty)/I_o$ or by double integration of the EPR signal area (A_o and A_∞), $E_L(\infty)$.

III. Theoretical Aspects

Before illuminating the sample all the molecules are in the A (bound) substate and contribute to the paramagnetic signal. During the illumination ligands are dissociating to the B unbound substate at a rate k_ν, which depends on the intensity of the lamp and on sample concentration . The ligands in the B substate do not contribute to the signal. We have searched for a wide line signal due to the dissociated NO ligands, but none was found. During the illumination some NO ligands return to the A substate with a reassociation rate k_L. After turning off the light a fraction of NO which remained in B, reassociates. This process is geminate and not exponential in time. During illumination the kinetics can be expressed as:

$$\frac{dF_B(t)}{dt} = k_\nu F_A(t) - k_L F_B(t) \qquad (2)$$

where $F_B = 1 - F_A(t)$ is the fraction of ligands in B. At $t = 0$, $F_A(0) = 1$ and $F_B(0) = 0$. Since $F_B(t) = F_L(t)$ the above equation becomes

$$F_L(t) = \frac{k_\nu}{k_\nu + k_L}\left\{1 - \exp\left[-(k_\nu + k_L)t\right]\right\} \qquad (3)$$

Since the light intensity during photolysis is relatively low, the kinetics are determined not only by k_ν, but also by the reassociation rate $k_L(E)$. This rate is given by the distribution of activation energies, $g(E)$. Eq. 2 becomes

$$F_L(t) = \int_0^\infty dE\, g(E) \frac{k_\nu}{k_\nu + k_L(E)}\left\{1 - \exp\left[-\left(k_\nu + k_L(E)t\right)\right]\right\} \qquad (4)$$

In steady state ($t \to \infty$) the dissociated fraction is given by

$$F_L(\infty) = \int_0^\infty dEg(E) \frac{k_\nu}{k_\nu + k_L(E)} \qquad (5)$$

The normalization of $F_L(t)$ gives

$$N_L(t) = \frac{\int_0^\infty dEg(E) \frac{k_\nu}{k_\nu + k_L(E)} \left\{1 - \exp\left[-\left(k_\nu + k_L(E)t\right)\right]\right\}}{\int_0^\infty dEg(E) \frac{k_\nu}{k_\nu + k_L(E)}} \qquad (6)$$

When equilibrium is established and the light is turned off the rebinding process is observed. The normalized fraction of ligands which remains in the B substate is then

$$N_D(t) = \int_{E_{min}}^\infty dEg(E) \exp\left[-k_D(E)t\right] \qquad (7)$$

where $k_D(E)$ is the reassociation rate in the dark and E_{min} represents the cut off in the energy distribution - the molecules with energy barrier below E_{min} having reassociated during illumination.

Since our measurements were made at temperatures below 20K, where the rebinding does not occur via classical over-the-barrier motion, the quantum-mechanical tunneling dominates. Among several tunneling models[13,14] we chose the

simplest one[1b] where

$$k_{L,D}(E) = A(T)\exp\left[-\gamma E^{\delta+1/2}\right] \qquad (8)$$

A(T) is the frequency factor, the exponential is the Gamow factor and δ is a free parameter, taken here equal to 1[1c]

For a parabolic barrier and $E >> K_B T$:

$$\gamma = \frac{\pi}{2h}(2M)^{1/2} d(E) \qquad (9)$$

where K_B is the Boltzmann constant, M is the reduced mass of Fe and NO and d(E) is the tunneling distance.

We follow Frauenfelder assuming that d(E) is the width at the bottom of the barrier and depends on the barrier height, E, through

$$d(E) = d_o\left(\frac{E}{E^p}\right)^{\delta} \qquad (10)$$

where d_o is the barrier width corresponding to the peak of the distribution energy, E^p.

Since it was shown[1b] that the principal parameters, E^p and A(T), do not depend on the choice of g(E), we used the energy distribution given by Alberding et al.[1c].

$$g(E) = g_o\exp\left\{\alpha(E^p - E) - n\exp\frac{\alpha}{n}(E^p - E)\right\} \qquad (11)$$

with $$\int_o^{\infty} g(E)dE = 1$$

where g_o is the normalization constant and α and n are adjustable parameters.

The parameters α, n, E^p, ACTD, d_o and k_ν were determined by Monte Carlo method minimizing the mean square error.

Assuming that the conformational substates are frozen at low temperatures the same distribution was used to fit the experimental curves in the dark. ACTD and d_o were left as free parameters and the energy E_{min} of the eq. 6, was introduced as another parameter.

Equation 5 was also fitted with the experimental values of $F_L(\infty)$ introducing a normalization constant N_o. The values of N_o and ACTD were obtained through an iterative process to obtain values of ACTD of the order of magnitude of the value obtained from the fit of $N_L(t)$.

IV. Results and Discussion

Figure 1 shows that the dissociation with light at 7.2K is considerable. S_o and S_∞ are EPR spectra of HbNO, before illumination and at equilibrium during illumination. After illumination in the new steady state, the resulting spectrum is very similar to S_∞ showing that the reassociated ligand fraction is quite small (8%). The kinetic curves $\Delta I_{L,D}(t)$ are shown in Figure 2. The fraction of dissociated ligands decreases from 0.82 at 5.3K to 0.26 at 15.5K. This fraction $F_L(\infty)$ differs by a factor of two from $E_L(\infty)$, obtained by double integration of the EPR signals. We believe that this is due to a difference in the

fraction of dissociated α and β chains, and possibly to the presence of R and T conformations which reflect differently on the EPR absorption area and on the amplitude of the signal in each situation.

The decrease of $F_L(\infty)$ with the increase of the temperature is due to a competition between k_ν, which is constant and the reassociation rate, $k_L(E)$, which increases with the temperature according to eq. 8. The kinetic curves can be observed only at temperatures T < 20K because of the limitations in signal to noise ratio.

The calculated values of A(T) are given in Figure 4 which shows that at temperatures below 7K, the pre-exponential factor A(T) is almost constant. The observed behaviour can be expressed by

$$A(T) = A_1 T^n + A_2 \exp(-\varepsilon/K_B T) \qquad (12)$$

where $A_1 = 291 s^{-1}$, $A_2 = 4.8 \times 10^{-4} s^{-1}$, $n = 0.59$ and $\varepsilon/K_B = 49.7 kJ/mol$. Similar behaviour was observed for CO in the β chains of Hb[1b].

The experimental results obtained under illumination with the normalized kinetic curve show that these curves do not depend on the temperature. The variation of $k_L(E)$ with T, is hidden by the effect of k_ν. Because of the normalization procedure, the temperature dependence observed in the Figure 2-a is lost. However for samples with concentration 8 times higher, which means a smaller k_ν, it becomes possible to observe temperature dependence of the normalized curves (Figure 5).

The parameters in Table 1 were obtained from the eqs. 5-11 using the model of conformational substates, in the tunneling regime. The energy distribution g(E) was obtained by fitting the experimental curves with the light on since the resolution is better than in the dark. At each temperature the curves were fitted separately and the sets of parameters obtained have nearly identical values. This confirms that the temperature dependence can be neglected. The final fitting was made from the average of the experimental points (Figure 3-a).

As shown previously[1b,c] in our case the Arrhenius rate parameter does not contribute to the observed kinetics.

Figure 3-b shows $N_D(t)$, the normalized kinetic curve in the dark. Since the recovery of the signal is small, energy distribution g(E) should not be determined from these results. The parameters of g(E) (α, n and E^p) obtained in the experiments with light, give a good fit to the kinetic results in the dark, only if d_o and A(T) are left free. It is also necessary to use a cut off in the energy distribution with a minimum energy E_{min} (Figure 6).

The tunneling parameter d_o is related to the peak energy of the distribution by eq.9. The difference between the values of d_o obtained from the kinetics with and without light is equivalent to a shift of the energy distribution[1d]. The effect of this variation is to decrease the reassociation rate in the dark in spite of the increase of the frequency factor A(T). To understand the meaning of these different tunneling barrier widths we can suppose that the light partially contributes favoring transitions to the excited states where the barrier width is smaller than that in the ground state (an intrinsic assumption of the model used

here). Another hypothesis is that the photolyzed molecules occupy more than one position[4c].

In our experiments the fastest ligands return during the illumination and correspond to a smaller tunneling distance, while the slower ones return in the dark and belong to conformations with larger tunneling distances.

For any given energy of the distribution g(E), $k_L(E)$ is much larger than $k_D(E)$. This characterizes two groups of molecules: fast (light on) and slow (light off). Since the dissociation rate k_ν is $0.07s^{-1}$ the ligands with $k_L(E) > 0.07s^{-1}$ can be rephotolyzed during the time of illumination, 120s. In the dark a small fraction of photolyzed ligands returns with slow rates while the major part is trapped in the pocket.

The kinetic curves can also be well fitted with a sum of two exponentials (Figure 7):

$$\text{Light on,}\quad N_L(t) = 1 - \left\{B_1\exp\left[-(k_{1L} + k_\nu)t\right] + B_2\exp\left[-(k_{2L} + k_\nu)t\right]\right\}$$

$$\text{Light off,}\quad N_D(t) = C_1\exp(-k_{1D}t) + C_2\exp(-k_{2D}t)$$

As can be seen in Figure 7, k_{1L} and k_{2L} are in the range of values determined for the fast group molecules by the previous model and k_{2D} for the slower group. A small fraction (10%) has a rebinding rate, k_{1D}, out of the range of the slower group and its value can be related to energy of 3.0kJ/mol, smaller than E_{min}. This may not be relevant in view of variety of the initial values of the various g(E) models for rebinding in the dark. In recent papers[15,16] it was shown that several distributions fit well the

experimental data in spite of their different initial energies. The k values of the sum of exponentials can be seen as dominant average rates given by the distribution model.

The E^p value of the distribution g(E) found here is 5kJ/mol. It is smaller than the value of E^p found for CO for carp-Hb[47]. Cornelius et al.[8a], in their picosecond photolysis work, found two geminate processes for NO ligand to Hb, at room temperature. They observed also that the geminate recombination of NO is faster than CO and occurs with greater probability, which led them to propose that the external barriers (to solvent) are the same for CO and NO and that the internal barrier is smaller for NO. Using low temperature experiments we were able to isolate the inner barrier and found E^p in a good agreement with their estimated value, without any assumption about the external barrier.

In the photolysis experiments with HbNO crystal[44] the estimated value of the activation energy was 7kJ/mol, which is within the distribution energy range found in this work. No tunneling has been observed. Nevertheless the temperature dependence shown in Figure 5 and the fitting of the experimental data strengthens the tunneling hypothesis.

Summarizing we have shown that the use of EPR at low temperatures leads to a coherent analysis of dissociation and reassociation kinetics of NO. These kinetics can be analyzed equally well by a conformational substate model, and by a superposition of two exponentials with different kinetic rates, k. Both dissociation and reassociation occur via tunneling only being limited to temperatures below 20K.

Acknowledgements. We are grateful to H.G.P. Lins de Barros, O.R. Nascimento, A.A da Gama and P.G. Wolynes for stimulating discussions and to E. Mavropoulos for the technical assistance in sample preparations.

Figure Captions

Figure 1 - EPR spectra of HbNO at 7.2K (0.2mM, phosphate buffer 0.1M, pH = 6.5). S_o, before photolysis and S_∞, at steady state during illumination; microwave power ≈ 0.2mW, modulation amplitude 2.0G.

Figure 2 - (a) $\Delta I_L(t)$ - fraction of dissociated NO under illumination; (b) $\Delta I_D(t)$ - fraction of dissociated NO in the dark; the gain of curves in (b) is twice that one in (a). HbNO 0.2mM, phosphate buffer 0.1M, pH =6.5.

Figure 3 - Normalized kinetic curves of HbNO (0.2mM, phosphate buffer 0.1M, pH = 6.5). $N_{L,D}(t)$ - normalized fraction of unbound NO: (a) light on: □ 9.2K, + 11.9K, ◇ 12.5K, Δ 13.8K; (b) light off: X 7.2K and 9.2K, ▽ 12.5K and 13.8K. The solid lines represent the fit with eqs. 4-10.

Figure 4 - The tunneling pre-exponential A(T) vs. log T; solid line represents the fit with eq. 5.

Figure 5 - Normalized kinetics of HbNO (1.2mM, phosphate buffer 0.1M, pH = 6.5) with light on: □ 11.7K, + 14.8K and ◇ 16.9K.

Figure 6 - Activation energy spectrum for innermost barrier in the

binding of NO to Hb. E_{min} is the energy cut off in the NO binding to Hb in the dark.

Figure 7 - Exponential model of normalized kinetic curves of HbNO. (a) light on (with $k_{\nu} = 0.07 s^{-1}$): $B_1 = 0.519$ $k_{1L}(s^{-1}) = 0.077$, $B_2 = 0.481$, $k_{2L}(s^{-1})$; (b) light off: $C_1 = 0.100$ and 0.652, $k_{1D}(s^{-1}) = 0.652$ and 0.914, $C_2 = 0.900$ and 0.835, $k_{2D}(s^{-1}) = 0.001$ and 0.001, for the curves at 7.2K and 9.2K and at 12.5K and 13.8K, respectively.

Table Caption

Table 1 - Parameters for NO Rebinding Process to Hb [a]

[a] Fitting parameters of the curves given in Figure 3 using the distribution function g(E): n = 0.3 and α = 1.6mol/kJ. [*] Log[A(s^{-1})] is 5.1 at 12.5K and 13.8K for curves in the dark. All other parameters are the same. [*] Not an adjusted parameter.

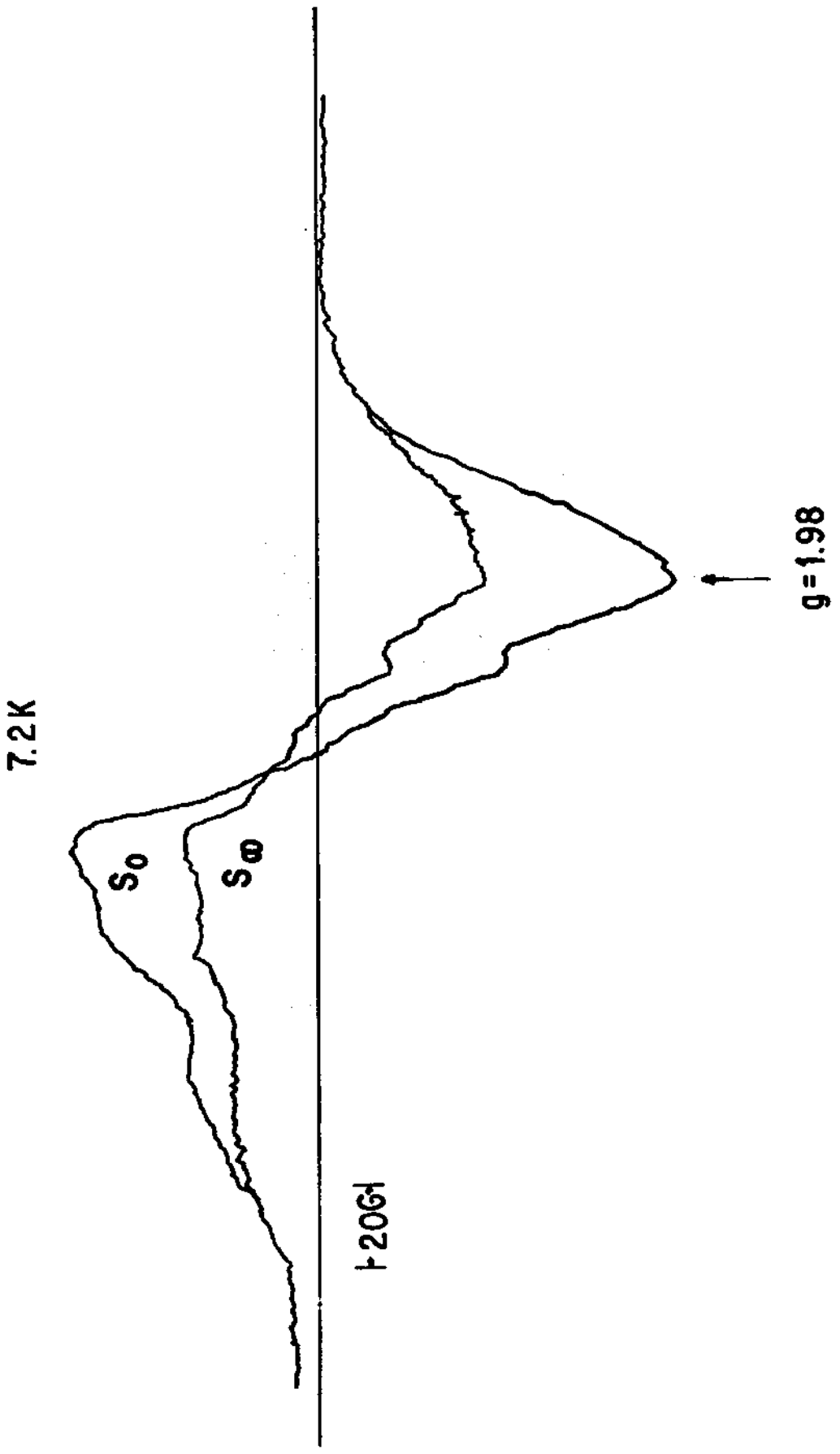

Figure 1

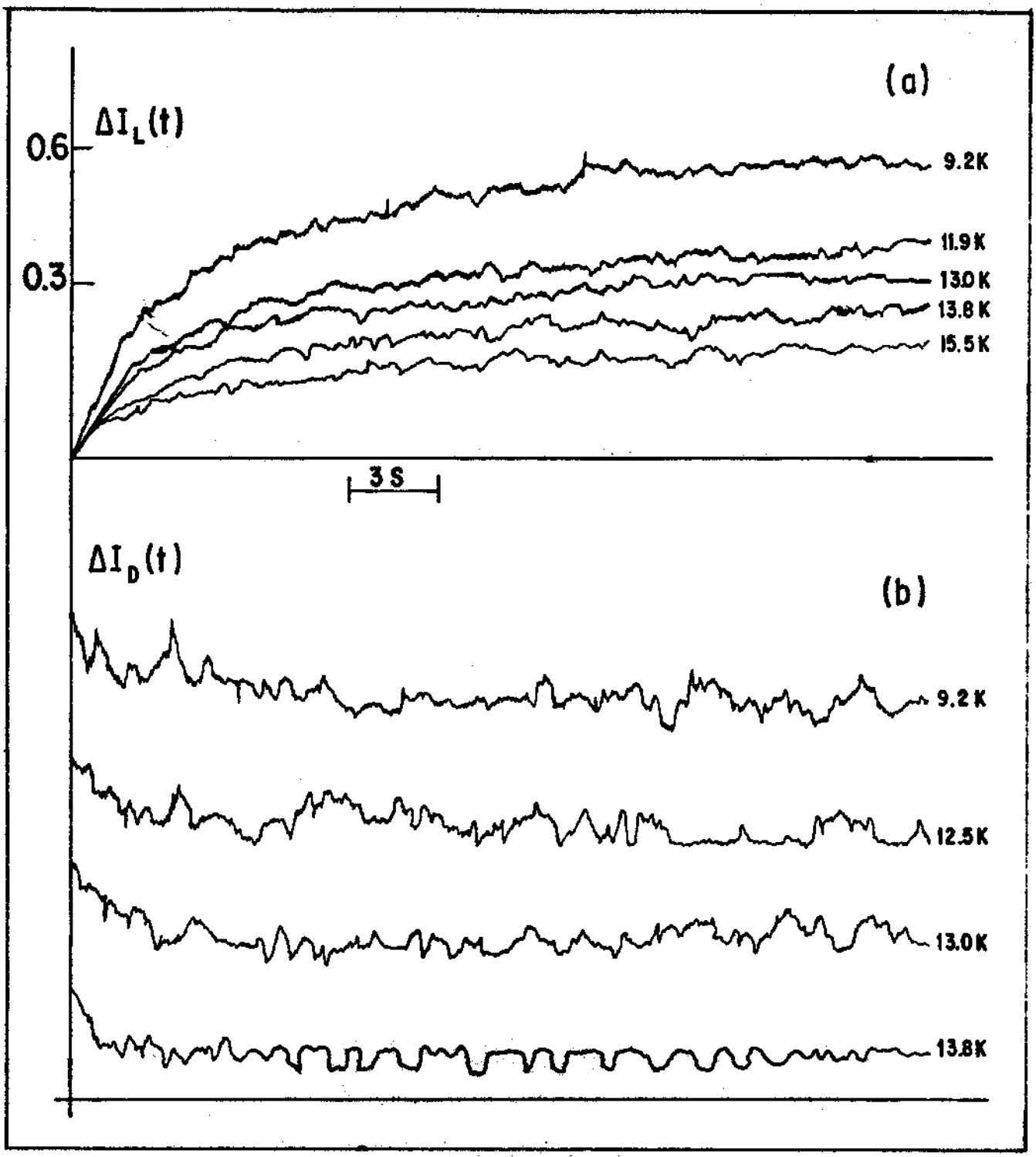
(a)
$\Delta I_L(t)$
0.6
0.3
9.2K
11.9K
13.0K
13.8K
15.5K
3 S
$\Delta I_D(t)$
(b)
9.2K
12.5K
13.0K
13.8K

Figure 2

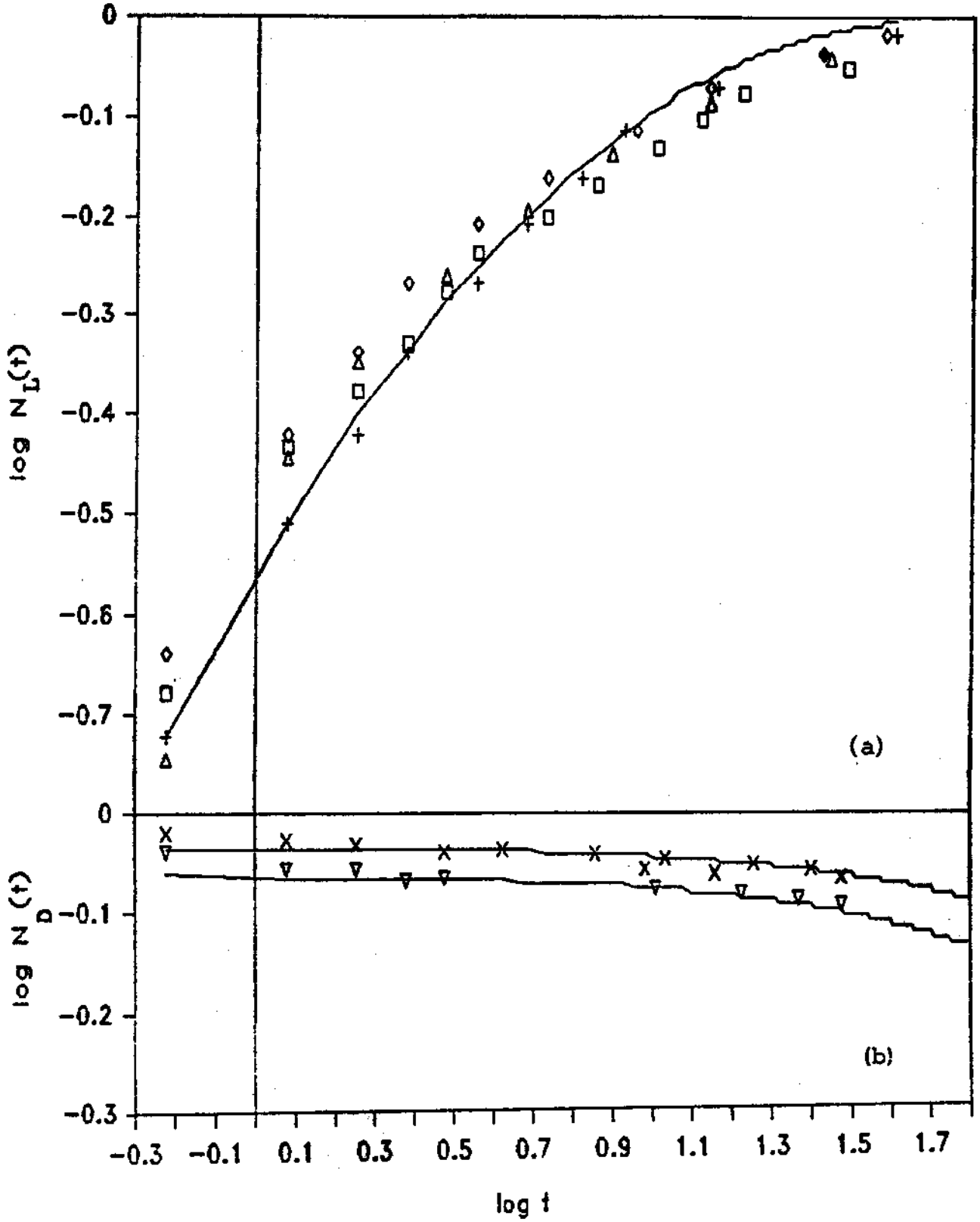
0
−0.1
−0.2
−0.3
−0.4
−0.5
−0.6
−0.7
log N_L(t)
(a)
0
−0.1
−0.2
−0.3
log N_D(t)
(b)
−0.3
−0.1
0.1
0.3
0.5
0.7
0.9
1.1
1.3
1.5
1.7
log t

Figure 3

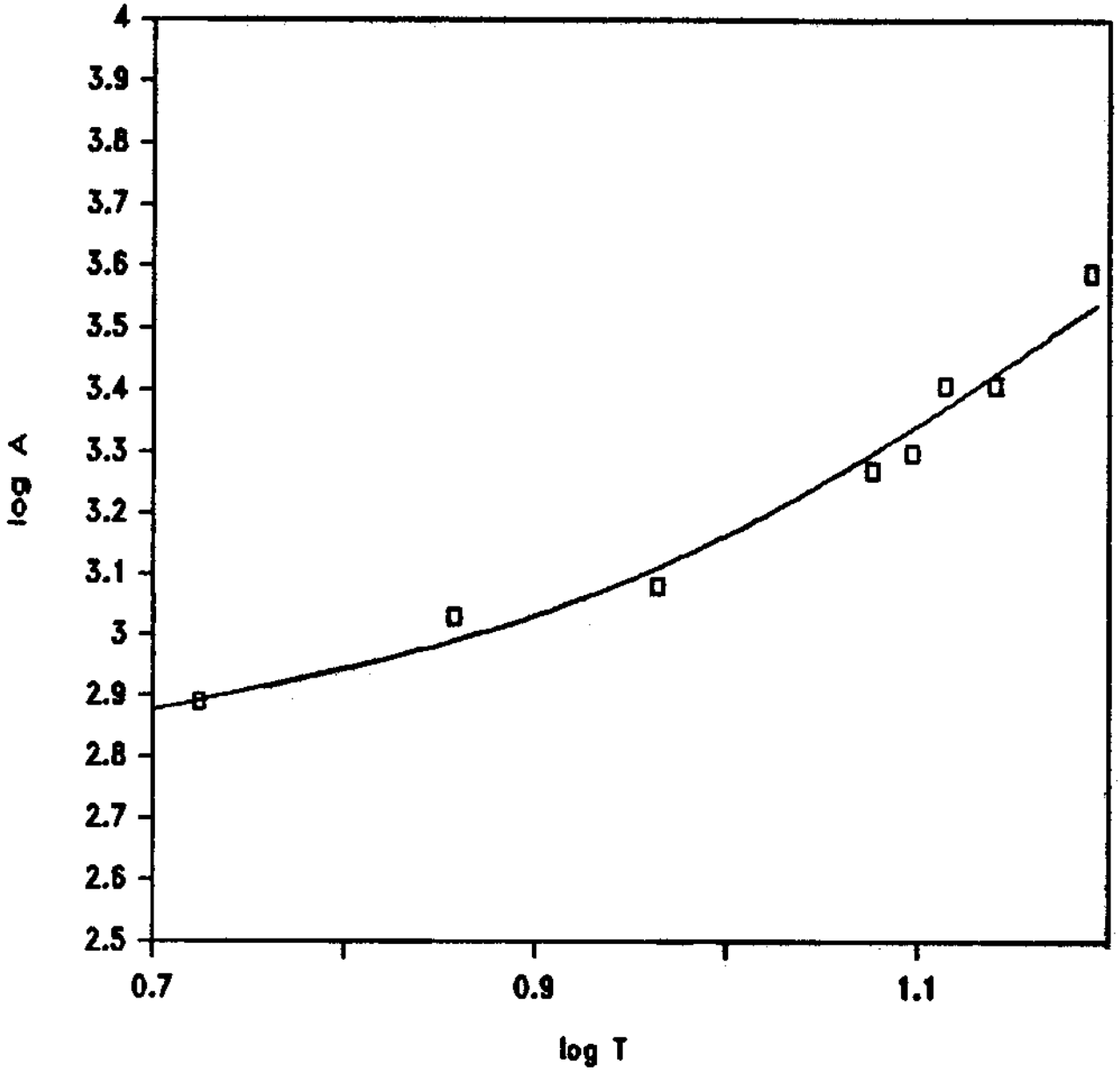

Figure 4

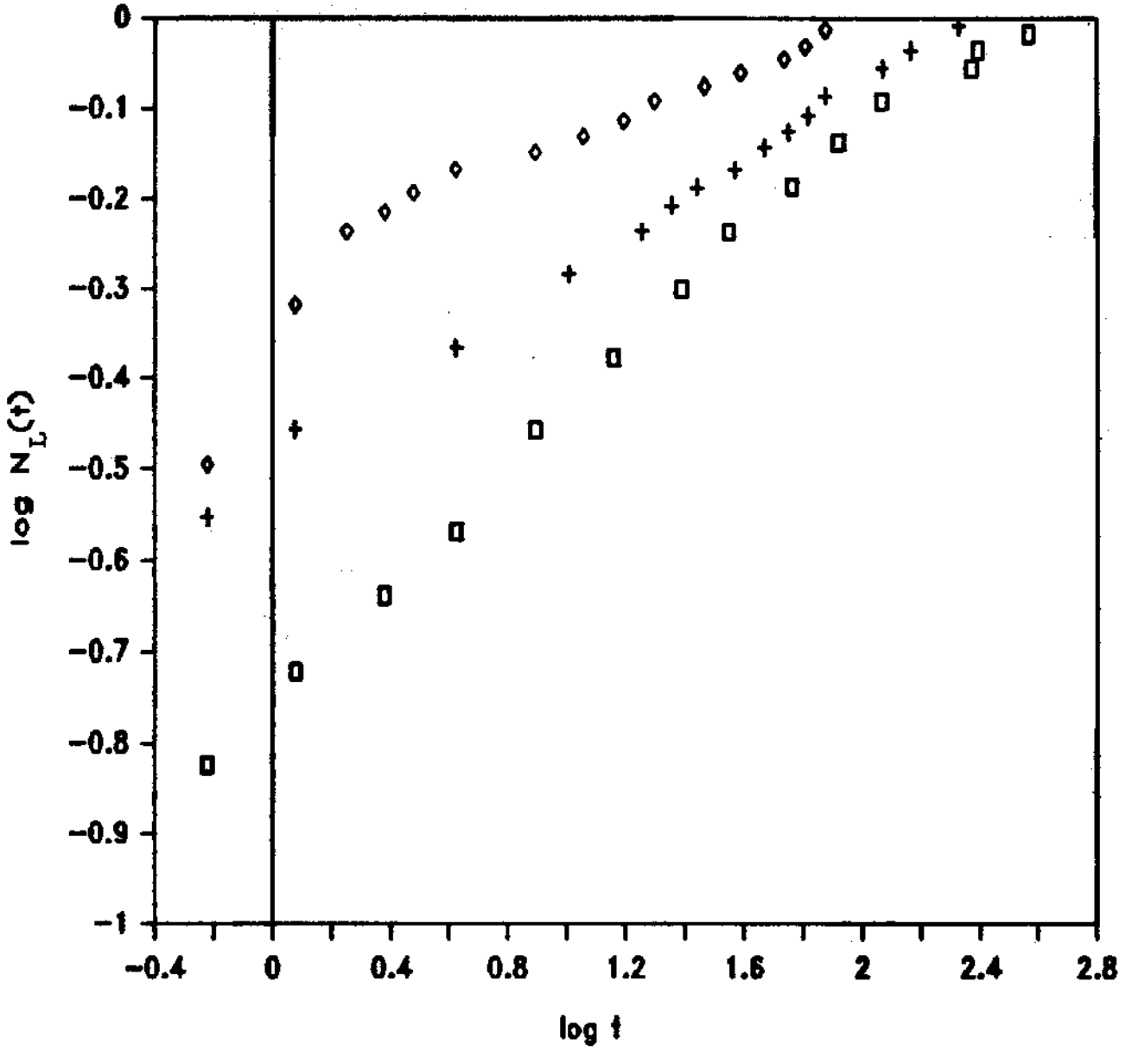

Figure 5

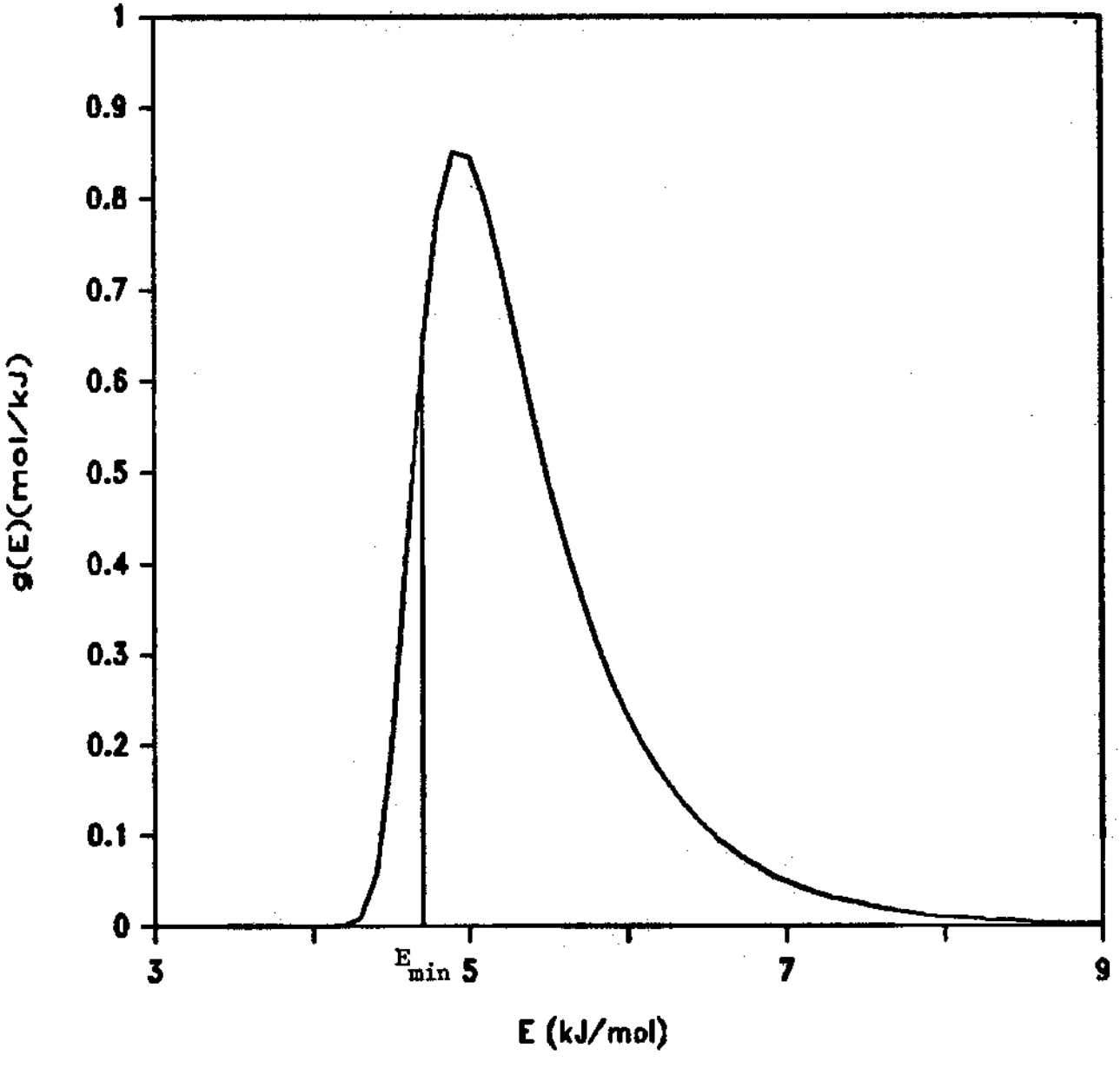

Figure 6

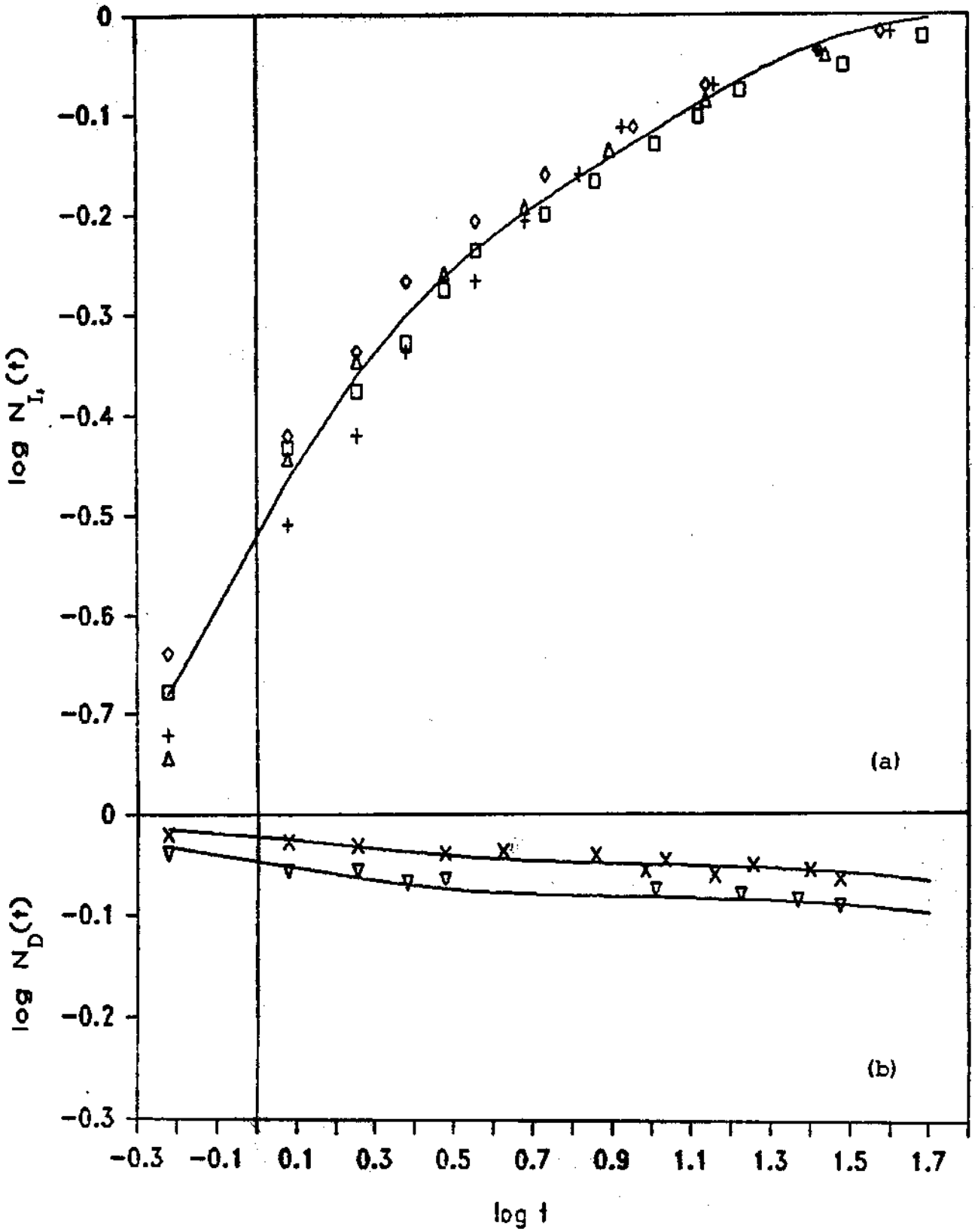
0
-0.1
-0.2
-0.3
-0.4
-0.5
-0.6
-0.7
log N_I(t)
(a)
0
-0.1
-0.2
-0.3
log N_D(t)
(b)
-0.3
-0.1
0.1
0.3
0.5
0.7
0.9
1.1
1.3
1.5
1.7
log t

Figure 7

	Light on	Light off
E^p(kJ/mol)	4.9	4.9
d_o(nm)	0.021	0.049
log[A(s^{-1})]	3.2	4.8*
k_v(s^{-1})	0.074	-----
E_{min}(kJ/mol)	4.4#	4.7
k_p(s^{-1})	1.8	0.36×10^{-2}

Table 1

References and Notes

(1) (a) Austin, R.H.; Beeson, K.W.; Eisenstein. L.; Frauenfelder, H.; Gunsalus,I.C. *Biochemistry* 1975,*14*,5355-5373. (b) Alberding, N.;Austin,R.H.;Beeson,K.W.; Chan,S.S.; Eisenstein, L.;Frauenfelder,H.; Nordlund,T.M. *Science* 1976,*192*,1002-1004. (c) Alberding,N.; Chan,S.S.; Eisenstein,L.; Frauenfelder,H.; Good,D.; Gunsalus,I.C.; Nordlund, T.M.; Perutz,M.F.; Reynolds,A.H.; Sorensen,L.B. *Biochemistry* 1978,*17*,43-51 (d) Ansari,A.; Berendzen,J.; Braunstein,D,; Cowen,B.R.; Frauenfelder,H.; Hong, M.K.; Iben,I.E.T.; Johnson,J.B.; Ormos,P.; Sauke,T.B.; Scholl,R.; Schulte,A.; Steinbach,P.J.; Vittitow,J.; Young,R.D.; *Biophysical Chemistry* 1987,*26*, 337-355. (e) Ormos,P.; Braunstein,D.; Frauenfelder, H.; Hong. M.K.; Lin, S.L.; Sauke, T.B.; Young, R.D. *Proc. Natl. Acad. Sci. USA* 1988,*85*,8492-8496.

(2) Goldstein,R.F.; Bialek,W.; *Comm. Mol. Cell. Biophys.* 1986, *3*(*5,6*),407-438.

(3) Murray,L.P.; Hofrichter,J.; Henry, E.R.; Eaton,W.A. *Biophysical Chemistry* 1988,*29*,63-76, recent review with other references.

(4) (a) Chance,B.; Fischetti,R.; Powers,L.; *Biochemistry* 1983,*22*, 3820-3829. (b) Powers.L.; Sessler,J.L.; Woolery, G.L.; Chance, B.; *Biochemistry* 1984,*23*,5519-5523. (c) Powers.L.; Chance,B.; Chance,M.; Campbell,B.; Friedman,J.; Khalid,S.; Kumar,C.; Naqui, A.; Reddy, K.S.; Zhou,Y. *Biochemistry* 1987,

26, 4785-4796. (d) Ondrias, M.R.; Friedman, J.M.; Rousseau, D.L. *Science* 1983, *220*, 615-617. (e) Rousseau, D.L..; Argade,P.V. *Proc. Natl. Acad. Sci. USA* 1986, *83*,1310-1314. (f) Campbell,B.F.; Chance,M.R.; Friedman, J.M. *Science* 1987, *238*, 373-376.

(5) (a) Hoffman,B.M.; Gibson,Q.H. *Proc. Natl. Acad. Sci. USA* 1978, 75,21-25. (b) Gibson, Q.H.; Hoffman, B.M. *J. Biol. Chem.* 1979, *254*, 4691-4697.

(6) Braunstein, D.; Ansari,A.; Berendzen,J.; Cowen,B.R.; Egeberg, K.D.; Frauenfelder,H.; Hong,M.K.; Ormos,P.; Sauke,T.B.; Scholl, R.; Schulte,A.; Sligar.S.G.; Springer,B.A.; Steinback,P.J.;Young, R.D. *Proc.Natl.Acad. Sci. USA* 1988, *85*, 8497-8501.

(7) Scholler,D.M.; Hoffman,B.M.; *J.Am. Chem. Soc.* 1979, *101*, 1655-1662.

(8) (a) Cornelius, P.A.; Hochstrasser, R.M.; Steele, A.W. *J. Mol. Biol.* 1983, *163*, 119-128. (b) Jongeward,K.A.; Marsters,J.C.; Mitchell,M.J.; Magde,D.; Sharma, V.S. *Biochem. Bioph. Res. Comm.* 1986, *140*, 962-966.

(9) (a) Louro, S.R.W.; Ribeiro, P.C.; Bemski,G. *Biochem. Biophys. Acta* 1981, *670*, 56-63 (b) Mun, S.K.; Chang. J.C.; Das, T.P.; *Proc. Natl. Acad. Sci. USA* 1979, *76*, 4842-4846. (c) Morse,R.H.; Chan,S.I. *J. Biol. Chem.* 1980, *255*, 7876-7882. (d) Hori,H.;

Ikeda-Saito, M.; Yonetani,T. *J. Biol. Chem.* 1981,*256*, 7849-7855.

(10) Nagai,K.; Hori,H.; Yoshida,S.; Sakamoto,H.; Morimoto,H.; *Biochem. Biophys. Acta.* 1978,*532*,17-18.

(11) Doetschman,D.C.; Utterback,S.G. *J. Am. Chem. Soc.* 1981,*103*, 2847-2852.

(12) LoBrutto,R.; Wei,Y.H.;Yoshida,S.; Van Camp,H.L.;Scholes,C.P.; King,T.E. *Biophys. J.* 1984,*45*,473-479.

(13) Frauenfelder,H. *Tunneling in Biological Systems*; B. Chance, D.C. DeVault, H. Frauenfelder, R.A. Marcus, J.R. Schrieffer, N. Sutin: Academic Press,1979; pp 827-846.

(14) Jortner, J.; Ulstrup,J. *J. Am. Chem. Soc.* 1979,*101*,3744-3754.

(15) El-Jaick,L.J.; Wajnberg,E.; Bemski,G.; Linhares, M.P. *Int. J. Biol. Macromol.* 1988,*10*,185-190.

(16) Plonka,A.; Kroh,J.; Berlin, Y.A. *Chem. Phys. Lett.* 1988, *153*, 433-435.

(17) Cobau,W.G.; LeGrange,J.D.; Austin, R.H. *Biophys. J.* 1985,*47*, 781-786.